JCB
J Circ Biomark 2026; 15: 69-77
ISSN 1849-4544 | DOI: 10.33393/jcb.2026.3797
ORIGINAL RESEARCH ARTICLE

Circulating free and low-density lipoprotein-bound GD2 can compete *in vitro* with neuroblastoma cells for binding therapeutic anti-GD2 antibodies

Christina S. Turn[1,2], Christine M. Busch[1], Cara Toland[1], Hamid Bassiri[2,3,4], Michael D. Hogarty[1,2], Frank M. Balis[1,2]

[1]Division of Oncology and Department of Pediatrics, Children's Hospital of Philadelphia, Philadelphia - USA
[2]Perelman School of Medicine at the University of Pennsylvania, Philadelphia - USA
[3]Division of Immunology, Johnson & Johnson Innovative Medicine, Spring House - USA
[4]Division of Infectious Diseases and Department of Pediatrics, Children's Hospital of Philadelphia, Philadelphia - USA

ABSTRACT

Introduction: GD2 is a ganglioside expressed on neuroblastoma cell membranes and shed into the circulation, where it primarily circulates bound to low-density lipoprotein (LDL). We questioned whether LDL-bound GD2 could interfere with the binding of therapeutic anti-GD2 monoclonal antibodies (like dinutuximab) to neuroblastoma cells.

Methods: The GD2-expressing neuroblastoma cell line IMR5 was stained with an anti-GD2 antibody tagged with allophycocyanin (APC) at the lowest possible saturating concentration, and mean fluorescence intensity was measured by flow cytometry after *in vitro* exposure to GD2-LDL or free GD2 at multiple concentrations. Control experiments assessed the ability of GD2-expressing and GD2-non-expressing cells to compete for anti-GD2-APC antibodies with IMR5 cells.

Results: Free and LDL-bound GD2 reduced anti-GD2-APC antibodies' binding to IMR5 cells *in vitro* in a concentration-dependent manner. At physiologically relevant concentrations, LDL-bound GD2 blocked antibody binding to IMR5 to a greater extent than free GD2, including at 100 nM, a concentration below median GD2 concentrations in patients with high-risk neuroblastoma. At higher concentrations, LDL-bound GD2 inhibited antibody binding to IMR5 by up to 92.6%, whereas the same concentration of free GD2 only decreased antibody binding by 56.6%

Conclusions: At concentrations found in patients with high-risk neuroblastoma, both free GD2 and LDL-bound GD2 blocked anti-GD2 antibody binding to neuroblastoma cells. These data suggest that circulating GD2-LDL could impact the efficacy of therapeutic anti-GD2 antibodies administered to patients with a high disease burden during induction therapy or at relapse and may have therapeutic implications for GD2-directed adoptive cellular therapies.

Keywords: Circulating GD2, Flow cytometry, GD2, Immunotherapy, Neuroblastoma

Introduction

GD2 is a disialoganglioside (glycosphingolipid) expressed on the surface of neuroblastoma tumor cells, and its exteriorized glycan domain is the antigenic target of the FDA-approved therapeutic anti-GD2 monoclonal antibodies dinutuximab and naxitamab (1-3). Dinutuximab is a component of frontline treatment regimens for high-risk neuroblastoma and is administered in the post-consolidation phase of therapy (3), when tumor burden is low. However, recent and ongoing clinical trials in the Children's Oncology Group and other pediatric oncology consortia are exploring the impact of administering dinutuximab in the induction phase of therapy. Dinutuximab and naxitamab are also effective in combination with chemotherapy for relapsed or refractory neuroblastoma (4,5).

GD2 is shed from the surface of neuroblastoma cells and is quantifiable in the serum and plasma of children with neuroblastoma at diagnosis (6). In a retrospective study, the median serum concentration of the C_{18}-lipoform of GD2 in children with high-risk neuroblastoma at diagnosis was 167 nM (7), which was 30-fold higher than the median GD2 concentration in healthy controls (8). Circulating GD2 concentrations in newly diagnosed neuroblastoma patients can range as high as 3 μM (unpublished data, communication with Frank Balis). However, patients who had completed induction and consolidation therapy have lower circulating GD2 concentrations (median 8.2 nM) (7). These data demonstrate

Received: April 23, 2026
Accepted: August 18, 2026
Published online: September 21, 2026

This article includes supplementary material

Corresponding author:
Christina S. Turn
email: turnc@chop.edu

that children with higher disease burden typically possess correspondingly elevated levels of circulating GD2. Although circulating GD2 has been posited as a potential biomarker for neuroblastoma, its effects upon GD2-targeting therapies are unknown.

In plasma, the majority of GD2 circulates as a complex with low-density lipoprotein (LDL). Ninety-eight percent of GD2 is LDL-bound in nonhuman primates (9), while humans' circulating GD2 is 73% bound to LDL and 21% bound to VLDL (10). Sialic acid moieties in the glycan domain of GD2 are ionized at physiologic pH and are likely to be oriented outward when bound to LDL rather than residing within the hydrophobic interior. Based on our finding of GD2 in the plasma of children with neuroblastoma (7), we hypothesized that this circulating GD2 could bind to therapeutic anti-GD2 antibodies and interfere with antibody binding to tumor cells. To confirm this hypothesis, we developed a novel *in vitro* method to assess competition between free or LDL-bound GD2 in the media and cell surface-bound GD2 for binding to a fluorescent anti-GD2 antibody. We demonstrated that anti-GD2 antibody binding to neuroblastoma cells is reduced in a concentration-dependent manner in the presence of free or LDL-bound GD2, suggesting that circulating GD2 could attenuate the efficacy of therapeutic anti-GD2 antibodies in patients with a high tumor burden or high concentrations of circulating GD2.

Methods

Cell Culture

IMR5 (RRID:CVCL_1306), a GD2-expressing neuroblastoma cell line, and RH30 (RRID:CVCL_0041), a GD2-nonexpressing rhabdomyosarcoma cell line, were grown in T75 flasks (surface area 75cm^2) with Roswell Park Memorial Institute medium (RPMI; Gibco, Grand Island, NY), supplemented with 10% FBS, 1% L-glutamine, 1% penicillin-streptomycin, and 0.05% gentamicin. Aseptic technique was employed with all cell handling procedures, and the cells were incubated at 37°C with 5% CO_2. Both cell lines' identities had previously been confirmed with short-tandem repeat analyses and with flow cytometry (most recently August 2025), and both cell lines tested negative for *Mycoplasma* (most recently August 2025). Both IMR5 and RH30 cell lines are derived from male pediatric patients, so sex was not an applicable variable in this study.

LDL and GD2 Solutions

A 500 µM stock solution of disialoganglioside GD_2 extracted from human brain (Cat # 345743 Calbiochem) was diluted in 80% methanol to make a 10x concentration solution for dilution to achieve the final desired concentrations of the GD2 in the media. GD2 was bound to LDL (Sigma Cat # L7914) by diluting the LDL in PBS to a final concentration of 0.8 mg/mL and adding 10x GD2 stock solution to achieve the desired GD2 concentration. Free (unbound) GD2 without LDL was made by adding the appropriate volume of 10x GD2 stock solution to PBS to achieve the desired GD2 concentration. All samples were vortexed for 5 minutes, then incubated for 30 minutes at 37 °C. GD2 binding to LDL was confirmed by passing the solution through a Vivaspin 500 filter with a 300 kDa molecular weight cutoff and measuring the concentration of GD2 in the filtrate with liquid chromatography-tandem mass spectrometry. The filtrate GD2 concentration was 15% of the total GD2 concentration in the starting solution; therefore, 85% of GD2 was bound to LDL, which is similar to the reported binding in human plasma (Supplemental Fig. 3).

Anti-GD2-APC Antibody Titration

As shown in Figure 1, these experiments were contingent upon the ability to detect changes in antibody availability to bind to GD2 or GD2-LDL. We employed the anti-GD2-allophycocyanin (anti-GD2-APC; RRID:AB_2563084; Cat # 357306, BioLegend, San Diego, CA) antibody, which is derived from the murine clone 14G2a. This is the same clone from which the therapeutic murine (m14.18), chimeric (dinutuximab, dinutuximab beta), and humanized (hu14.18K322A) antibodies were derived, and it recognizes the same epitope. Naxitamab, the other FDA-approved humanized anti-GD2 antibody, comes from a different hybridoma clone (3F8) and avidly targets a smaller epitope on GD2's exteriorized five-sugar residue. Its increased avidity and narrower target suggest that the anti-GD2-APC antibody employed in our experiments would also provide some insight into naxitamab's capacity to bind circulating GD2.

Anti-GD2-APC was titrated to identify the lowest concentration of antibody that saturated binding epitopes, such that any further reduction in antibody concentration would result in reduced detection of fluorescence and decreased positive/negative population discrimination. GD2-positive IMR5 cells were stained with varying concentrations of anti-GD2-APC (250 ng, 125 ng, 62.5 ng, and 31.25 ng per million cells) according to in-house protocols (11), and fluorescence was evaluated on a MACSQuant cytometer (RRID:SCR_020268; Miltenyi Biotech, Bergisch Gladbach, Germany). At least 150,000 events were recorded for each sample, and three biological replicates were collected for each experimental condition. The stain index was calculated for each concentration (Fig. 2), and the antibody concentration of 125 ng per million cells was selected for all subsequent experiments. We used the same antibody concentration for an anti-IgG2-APC isotype as a control measure (RRID:AB_3097080; Cat #403608 Biolegend, San Diego, CA).

Free GD2 and LDL-bound GD2 Exposure and Preparation for Flow Cytometry

Cells were grown simultaneously in parallel flasks, one for each of three biological replicates. IMR5 cells were dissociated from the flask, pelleted, and washed in PBS three times prior to suspension in 1% BSA in PBS during processing. Two million cells per condition were aliquoted into flow cytometry tubes. Cells were prepared for flow cytometry as done previously (11) and were first stained with Live/Dead Fixable Aqua Stain (1 µL per million cells, Biolegend) prior to incubation on ice. After washing excess/residual stain from the cells, TruStain fcX (Cat # 422301, Biolegend) was added for 15 minutes on ice to block Fc receptors and indiscriminate binding.

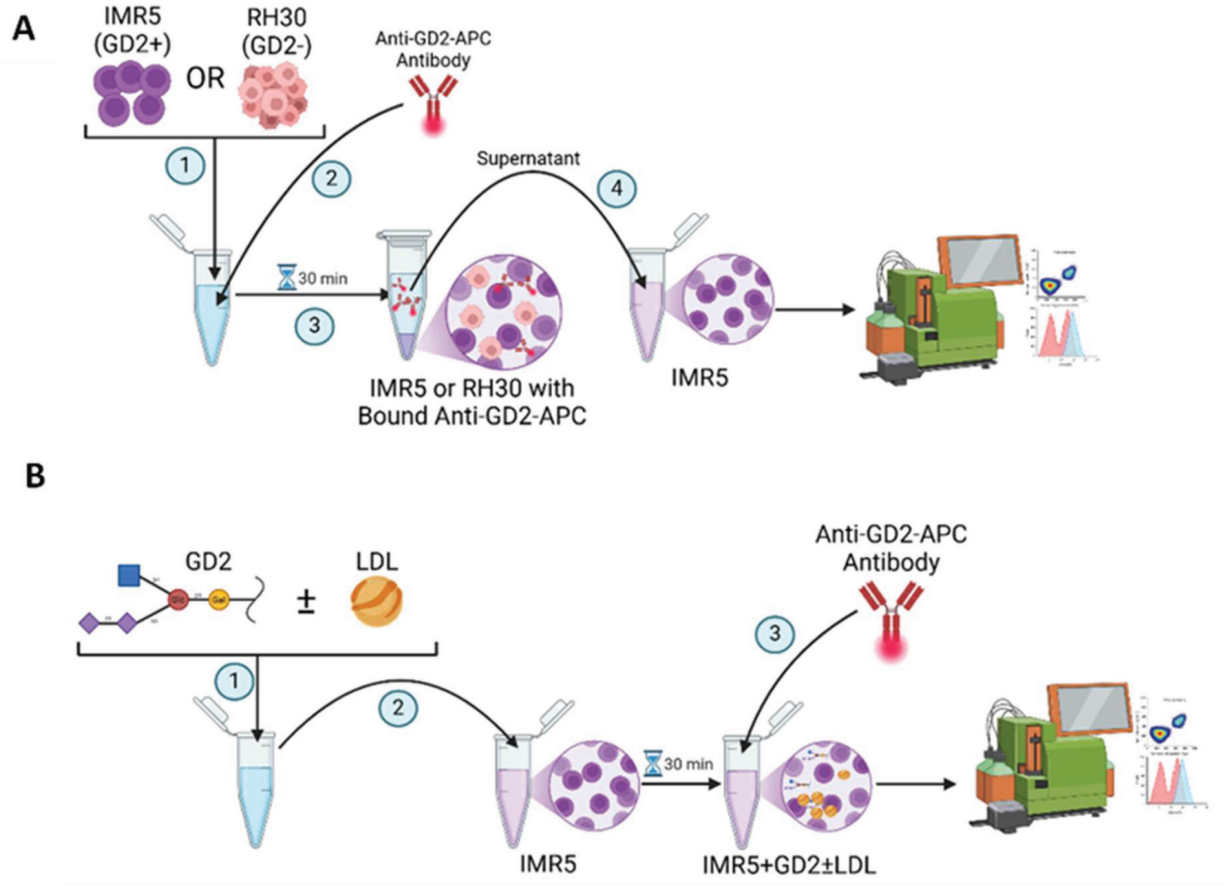

FIGURE 1 - *In vitro* determination of direct competition for anti-GD2 antibodies. A) Control experiments assessed the ability of cellular GD2 on IMR5 cells to capture anti-GD2-APC antibodies and to prevent them from binding to the test IMR5 population. GD2-non-expressing RH30 cells were employed as a negative control. Anti-GD2-APC antibodies were incubated with either IMR5 or RH30 cells for 30 minutes before centrifugation, and remaining antibodies in the supernatant were then utilized to stain IMR5 cells for enumeration by flow cytometry. B) GD2 molecules were placed in solution, either with or without prior complexing with LDL. The GD2 mixture was added to IMR5 cells, and together they were incubated with anti-GD2-APC antibodies. The solution was centrifuged so that circulating GD2 was removed, and the stained IMR5 cells were evaluated with flow cytometry. Figure created with BioRender.

The cells were rinsed prior to the application of exogenous free GD2 (concentrations: 0 nM, 100 nM, 1 µM, and 5 µM) or LDL-bound GD2 (concentrations: 100 nM, 1 µM, and 5 µM of GD2). Cells were placed on a rotary shaker and incubated on ice for 15 minutes and then at room temperature for 15 minutes prior to being stained with the anti-GD2 conjugated fluorophore (anti-GD2-APC, 2.5 µL [125 ng] per million cells, Cat # 357306, Biolegend). The stained cells were washed and pelleted prior to processing via flow cytometry. Negative control beads (Cat # 01-1111-41, Invitrogen) were employed for anti-GD2-APC compensation.

Preparation of Control Cellular Suspensions

IMR5 and RH30 cells were dissociated, harvested, and suspended in PBS with 1% BSA as above. To determine if there are differences between exogenous GD2 and membrane-bound GD2 uptake of the anti-GD2 antibody, anti-GD2-APC antibody was applied to populations of RH30 (2 million cells) or IMR5 (2 or 4 million cells) and incubated for 30 minutes on a rotary shaker (15 minutes on ice, 15 minutes at room temperature). The cells were then centrifuged at 1200 rpm at 4°C for five minutes, and the resultant supernatant, devoid of anti-GD2-APC antibody bound to the surface of the tumor cells, was collected and applied to samples of IMR5 cells that had already been stained with viability dye and Fc blockade as above.

Flow Cytometry and Data Analysis

All control and experimental samples underwent flow cytometry utilizing a MACSQuant cytometer, evaluating 500,000 events per condition for the GD2/LDL study and 150,000 events per condition for the cellular control experiments. FlowJo software (RRID:SCR_008520; v. 10.10; TreeStar, Ashland, OR) was employed with in-house standard gating protocols for all analyses (11). Gating strategies are detailed in Supplemental Figure 1.

Mean fluorescence intensity (MFI) was defined by the geometric mean in each experiment. To minimize variance among flow cytometry runs, all MFIs were normalized using the MFI of negative, unstained cells collected on each day. The normalized MFIs of each experimental group were then compared to untreated, stained IMR5 cells using a lognormal, one-way Welch's ANOVA with *post-hoc* Dunnett's multiple comparison tests. For all statistical tests, the α was set at 0.05. Data analysis was completed in Excel (Microsoft, Seattle, WA) and Prism (RRID:SCR_002798; GraphPad, San Diego, CA).

Results

GD2-Expressing Cells Bind Fluorescently Tagged Anti-GD2 Antibody

We identified the lowest concentration of anti-GD2-APC antibody that would achieve epitope saturation without leaving excess, unbound antibody. The selected antibody concentration (125 ng per million cells) stained membrane-bound GD2 on IMR5 cells without excess anti-GD2-APC; lower concentrations were unable to discriminate between GD2+ and GD2- populations (Fig. 2). As a control measure, we confirmed that our neuroblastoma cell line, IMR5, had detectable, membrane-bound GD2 and that our negative control rhabdomyosarcoma cell line, RH30, did not. As expected, IMR5 cells demonstrated a robust MFI, whereas RH30 cells showed minimal fluorescence (Fig. 3).

In children, therapeutic anti-GD2 antibodies bind to cell membrane-bound GD2 presented on the surface of neuroblasts and peripheral nerve fibers. Therefore, we next validated our *in vitro* assay to detect changes in fluorochrome-labeled anti-GD2 antibody concentrations in response to competition from surface-expressed GD2 on IMR5 cells. Suspensions of IMR5 and RH30 cells were exposed to anti-GD2-APC antibody for 30 minutes while on a rotary shaker, followed by centrifugation and collection of the supernatant containing the remaining, unbound antibody (Fig. 1A). The supernatant containing this remaining, fluorophore-tagged antibody was then applied to 2×10^6 IMR5 cells and enumerated with flow cytometry. When IMR5 cells were incubated with the supernatant from RH30 cells that were exposed to anti-GD2-APC antibody, the average MFI of the IMR5 cells was not significantly lower than IMR5 cells primarily exposed to anti-GD2-APC antibody (normalized mean IMR5 = 150.7 ± 27.9; normalized mean RH30-exposed IMR5 = 123.0 ± 169.4; Figs. 3A-B). However, two of three biological replicates did have lower MFIs than IMR5 alone, while the third had a population of more intense staining. This MFI reduction most likely represents antibody loss due to non-specific entrapment among cells during centrifugation and washing steps, but overall, this control experiment demonstrates that MFI shifts in other experiments are unlikely to arise from non-specific binding.

Low (2×10^6) and high (4×10^6) numbers of IMR5 cells were also exposed to anti-GD2-APC antibody, and the supernatant containing the remaining unbound antibody was collected (Fig. 1A). The supernatants were then applied to 2×10^6 IMR5 cells, and anti-GD2-APC antibody binding was assessed by flow cytometry (Figs. 3C-D). The MFIs were substantially

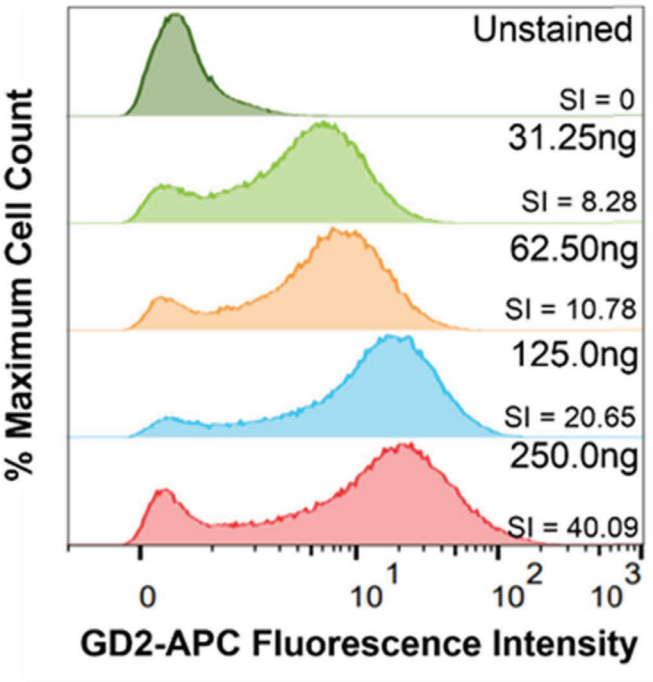

FIGURE 2 - Anti-GD2-APC Antibody Titration. Varying concentrations of anti-GD2-APC were applied to samples of IMR5 cells to identify the lowest concentration that would facilitate positive and negative population discrimination. Utilizing this concentration would avoid unnecessary oversaturation of samples with antibody in subsequent experiments and would allow the detection of any shifts in staining intensity secondary to competition between cell-bound and free GD2. Concentrations of anti-GD2-APC per million cells are listed on the right. Due to the preserved peak fluorescence observed at 125 ng per million cells and separation of positive and negative populations, this antibody concentration was employed for further experiments. SI = Staining Index.

lower in the IMR5 cells exposed to the supernatants from the low and high IMR5 groups compared to the IMR5 control group that was primarily exposed to anti-GD2-APC (Figs. 3C-D) or exposed to anti-GD2-APC pre-incubated with RH30 cells. The MFI of the cells exposed to the supernatant from the low group was 63.2 ± 56.7, compared to 150.7 ± 27.9 in the IMR5 control group, and the cells exposed to the supernatant from the high group had an MFI of 28.9 ± 31.8. Welch's one-way ANOVA with Dunnett's multiple comparison testing demonstrated that the high IMR5 group had significantly less fluorescence intensity than IMR5 cells alone, while the low IMR5 group did not have a statistically significant decrease.

Together, these experiments demonstrated that this *in vitro* flow cytometry assay can quantify the effect of labeled anti-GD2 antibodies being sequestered by cell surface-presented antigens, as evidenced by a shift in MFI.

LDL-Bound and Free GD2 Directly Compete with Membrane-Bound GD2

After establishing that the assay could quantify antibody competition by membrane-bound GD2, we assessed the ability of free or LDL-bound GD2 in suspension to bind anti-GD2

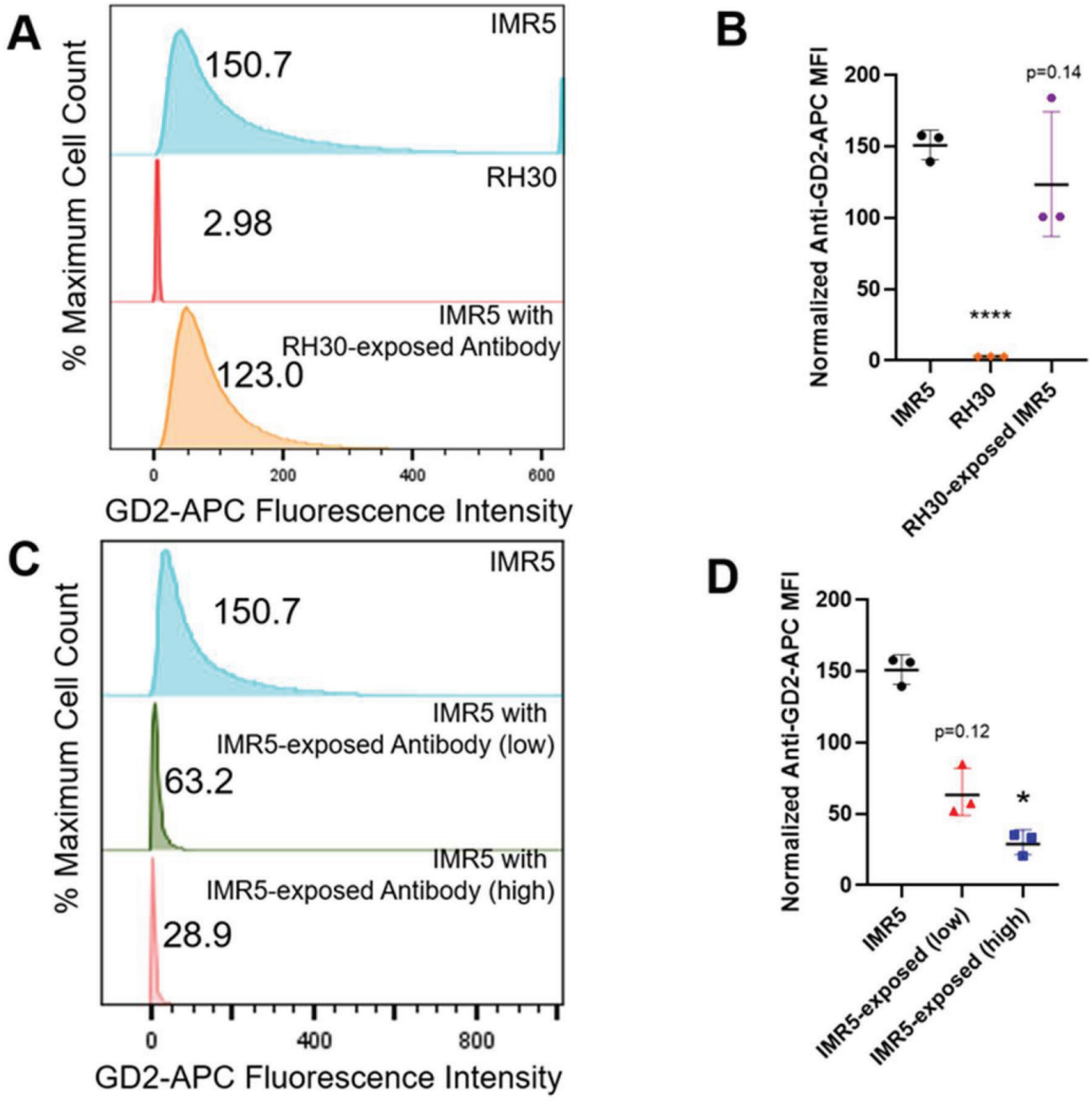

FIGURE 3 - Mean fluorescence intensity of IMR5 cells stained with cell-exposed anti-GD2-APC. A) GD2-expressing IMR5 cells demonstrated a normalized mean fluorescence intensity (MFI) of 150.7, while GD2-negative RH30 cells had a much lower MFI. B) IMR5 cells stained with antibodies exposed to a matched population of RH30 cells did not show a statistically significant MFI decrease. C) IMR5 cells stained with anti-GD2-APC exposed to an equal population (2×10^6; low) of IMR5 cells showed a non-significant shift in MFI, which was enhanced in cells stained with antibody exposed to a population of 4×10^6 (high) IMR5 cells. Panels B and D show the normalized MFIs of each biological replicate, along with their average MFI and standard deviation, based on the total enumerated cells (at least 150,000 events per biological replicate). Statistical significance was assessed with a log-transformed Welch's one-way ANOVA with *post hoc* Dunnett's testing. * = $p < 0.05$, **** = $p < 0.00001$ compared to IMR5 control.

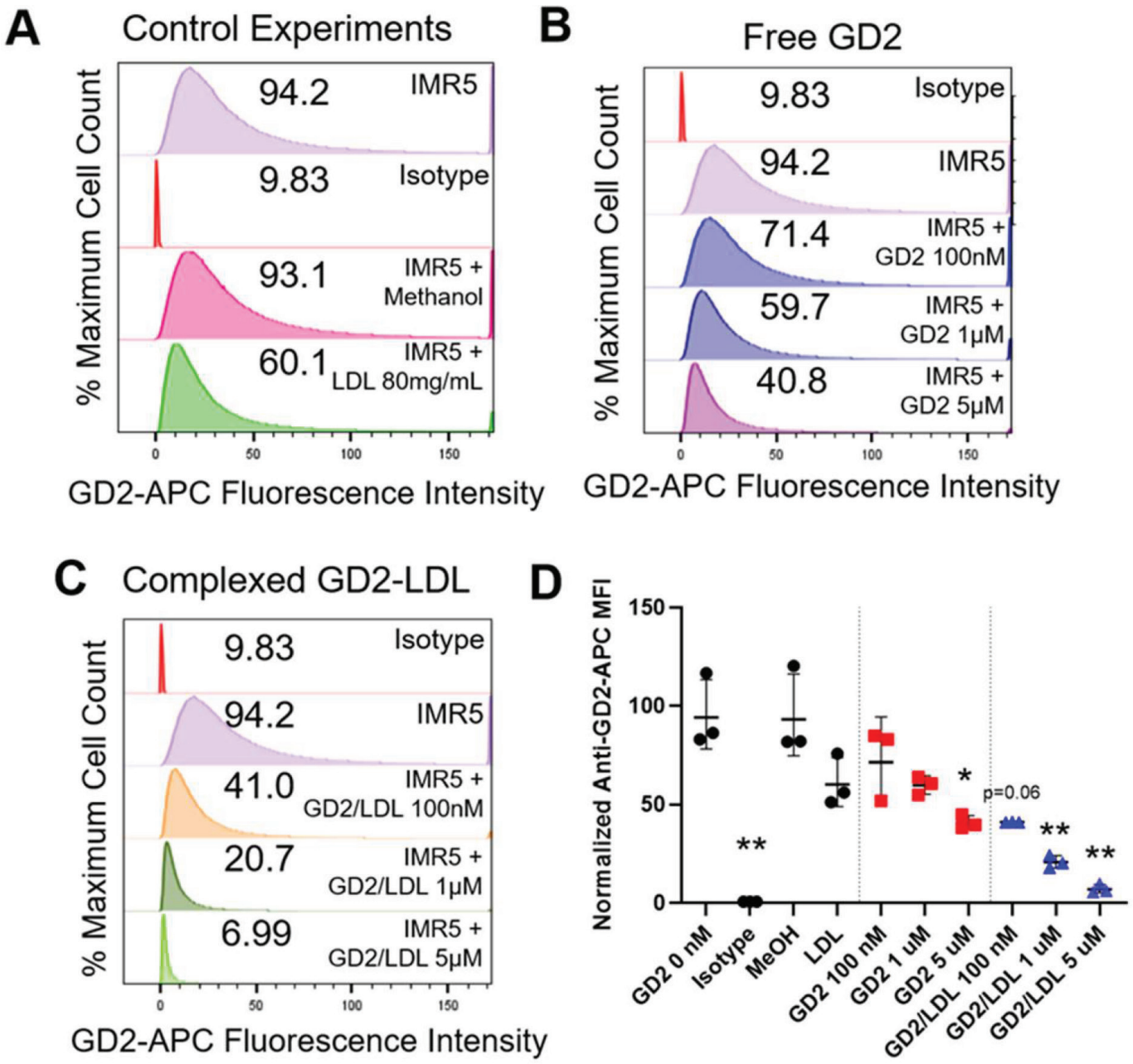

FIGURE 4 - Both free and LDL-complexed GD2 shift the MFI of anti-GD2 stained IMR5 cells. A) IMR5 cells were stained with anti-GD2-APC or anti-IgG2a-APC isotype. Two groups of IMR5 cells were mixed with either methanol or LDL to account for any MFI changes related to these carriers. Neither methanol nor LDL significantly decreased MFI. B) IMR5 cells were mixed with varying concentrations of free GD2 prior to staining with anti-GD2-APC. Free GD2 molecules (with any bound antibodies) were then removed via centrifugation. A statistically significant leftward shift in MFI was observed with the highest free GD2 concentration, showing a decrease in antibody availability. B) IMR5 cells were mixed with one of three concentrations of GD2-LDL complexes prior to staining and processing. These samples demonstrated a decrease in antibody availability inversely correlated with higher GD2 concentrations. Each curve represents concatenated data from 3 biological replicates. A-C) Each curve represents concatenated data from 3 biological replicates with the average MFI displayed. D) This summary bar graph demonstrates the MFIs and standard deviation for each tested group, stratified according to concentration of GD2. To determine statistical significance, the geometric means/MFI of each sample underwent log-transformed Welch's one-way ANOVA with Dunnett's *post hoc* intergroup testing. * = $p < 0.05$, ** = $p < 0.01$ compared to the 0nM control.

antibodies, thereby reducing effective fluorophore staining of IMR5 cells. Most GD2 circulates in the bloodstream bound to LDL. We therefore completed these experiments with either LDL-bound GD2 or free GD2 at concentrations ranging from 100 nM, which is slightly below the median plasma concentration in children with high-risk neuroblastoma, to 5 µM, which is higher than the upper range (approximately 3 µM) detected in children with high-risk neuroblastoma at diagnosis (unpublished data; communication with Frank Balis) (Fig. 1B).

The LDL-complexed GD2 suspensions included both LDL and a small quantity of methanol (MeOH). We first confirmed that neither LDL nor MeOH significantly disrupted anti-GD2 binding in this *in vitro* assay (Figs. 4A & D). The lowest concentration tested (100 nM) did not statistically affect IMR5's MFI in the free GD2 exposure group. Although the 100 nM LDL-bound GD2 group did not achieve statistical significance ($p = 0.06$), the large effect size may still have clinical significance. Free and LDL-bound GD2 in suspension at the highest concentration both decreased the MFI of anti-GD2-stained IMR5 (Figs. 4B-C), and LDL-bound GD2 demonstrated a statistically significant, concentration-dependent decrease in anti-GD2 binding to IMR5 cells compared to IMR5 control cells ($p < 0.01$ for 1 µM and 5 µM; Fig. 4D) and IMR5 cells with LDL-only ($p < 0.0001$ for 1 µM and 5 µM). The 5 µM GD2 concentration demonstrated a 56.6% decrease in MFI for free GD2 ($p < 0.05$) and a 92.6% decrease for LDL-bound GD2 ($p < 0.01$; Fig. 4). Interestingly, the physiologically relevant form of GD2 complexed to LDL more effectively competes with membrane-bound GD2 for antibodies than free GD2.

Discussion

We demonstrate that circulating GD2 has the capacity to bind anti-GD2 antibodies and to compete with antibody binding to GD2-expressing tumor cells. This direct competition is seen with both free and LDL-bound GD2, which demonstrates that the complexing of GD2 with LDL does not alter or mask the GD2 epitope recognized by such antibodies. Instead, physiologic concentrations of LDL-complexed GD2 demonstrate enhanced binding affinity to anti-GD2 antibodies. Additionally, we show that such binding of anti-GD2 antibody to circulating GD2 reduces antibody binding of GD2-expressing neuroblastoma cells in a dose-dependent fashion in this assay in which antibody concentration is not far in excess of available binding sites.

Children with newly diagnosed high-risk neuroblastoma have substantially higher circulating concentrations of GD2 compared to healthy controls, as measured by high-pressure liquid chromatography tandem mass spectrometry (LC-MS/MS) (7,8). In a cohort of 680 healthy children ranging from infancy to greater than 10 years of age, the median circulating GD2 concentration was 8.3 nM (range <3.0 nM to 94.8 nM), with children aged 6-12 months exhibiting a higher median of 18.0 nM (range <3.0 nM to 94.8 nM) (8). Healthy children aged 1-3 years demonstrated a lower median (11.6 nM) and maximum GD2 concentrations (38.0 nM), and circulating GD2 concentrations decreased further in older children (8). In contrast, children diagnosed with high-risk neuroblastoma (largely greater than 1 year of age at the time of evaluation) demonstrated much higher plasma GD2 concentrations in a retrospective study (7). At the time of diagnosis, children with low- and intermediate-risk neuroblastoma had a median GD2 concentration of 20.6 nM, compared with the control median of 5.6 nM in that study (7). Seventy-three individuals with high-risk disease, however, possessed higher concentrations of GD2 (median 167 nM, maximum 1060 nM) (7). An additional retrospective cohort of high-risk neuroblastoma patients showed maximum C_{18} GD2 concentrations of about 2000 nM (12). Circulating GD2 concentrations decrease at variable rates during induction chemotherapy, as seen in patients whose GD2 levels were assessed post-consolidation (median 8.2nM) and prior to initiation of immunotherapy (7,12) and to similar levels both pre- and post-immunotherapy (12). However, these circulating GD2 concentrations tend to rise at relapse (12).

Therapeutic anti-GD2 antibodies are part of standard, up-front treatment for high-risk neuroblastoma. Several anti-GD2 monoclonal antibodies currently exist, but the most commonly used (dinutuximab, hu14.18K322A, and mu14.18) are derived from the same m14G2a hybridoma clone that generated the anti-GD2 antibody used in this *in vitro* assay and therefore share the same epitope. Other anti-GD2 antibodies like naxitamab are derived from the 3F8 clone and thus have a smaller epitope on GD2's extracellular surface and also bind it more avidly (13). However, GD2's non-membranous domain only consists of five sugar residues, whereas the maximum size of any carbohydrate epitope is six or seven residues (14). Therefore, we expect that these *in vitro* results should provide valuable insight into circulating LDL-GD2 complexes' competition for anti-GD2 antibodies from either the m14G2a or m3F8 clones.

In standard-of-care regimens, anti-GD2 antibodies are currently administered in the post-consolidation phase at the end of therapy, when tumor burden and circulating GD2 concentrations are low and when peak serum antibody concentrations can be between 6 and 15 µg/mL after four daily infusions (15). These antibodies have also proven to be efficacious when combined with chemotherapy (like irinotecan and temozolomide) in the relapse setting, which can also be associated with elevated circulating GD2, although tumor burden at relapse is typically lower than at initial diagnosis (7,12). The optimal timing of administration of this effective immunotherapy continues to be evaluated.

Children's Oncology Group studies ANBL17P1 (NCT03786783) and ANBL2131 (NCT06172296) are assessing whether administering dinutuximab with induction chemotherapy will enhance the overall survival of children with high-risk neuroblastoma, and a similar trial involving naxitamab is accruing subjects (NCT05489887). Additionally, a phase 2 study evaluating the up-front use of the humanized anti-GD2 antibody hu14.18K322A starting in induction was well-tolerated and has improved both three-year overall and event-free survival (86.0% and 73.7%) (16, 17). This phase 2 study found that median peak antibody serum levels directly correlated with early response to treatment, thus demonstrating that higher antibody concentrations during times of presumably higher circulating GD2 are also associated with better outcomes (17).

In many adult cancers, the efficacy of therapeutic monoclonal antibodies, such as rituximab (anti-CD20), pembrolizumab (anti-PD-1), and atezolizumab (anti-PD-L1), directly correlates with the amount of antigen expressed on malignant cells (18-21). However, the presence of increased soluble PD-L1 at the time of diagnosis correlates with inferior therapeutic responses to anti-PD-L1 antibodies/immune checkpoint blockade in multiple solid malignancies in adults (22-24). High soluble PD-L1, defined as approximately 300-500 pg/mL (approximately 9-15 picomolar) (24), is greatly exceeded by the circulating GD2 concentrations found in patients with neuroblastoma. Therefore, moving neuroblastoma immunotherapy to induction will mean that some participants may receive anti-GD2 antibodies while they have both high amounts of cell surface-presented GD2 and elevated plasma concentrations of circulating LDL-bound GD2. During this time, when the ratio of anti-GD2 antibody to cell-bound GD2 target is lowest, our data suggest that this subset of patients may not derive the full benefit of dinutuximab despite incurring the same risks of dinutuximab toxicity, including anaphylaxis, neuropathic pain, and capillary leak syndrome. Binding of anti-GD2 antibodies to circulating GD2 could also enhance toxicities mediated by complement activation. We posit that the timing of administration of chemoimmunotherapy in induction or in initial relapsed disease could be guided by pretherapeutic measurements of circulating GD2 as a biomarker to ensure that anti-GD2 therapies effectively bind to neuroblastoma cells rather than binding to off-target, circulating GD2.

Our *in vitro* study attempts to model a clinically important scenario related to the impact of binding of therapeutic antibody to cell-free, circulating antigen. Circulating GD2 is being investigated as a diagnostic and prognostic circulating tumor biomarker for neuroblastoma and is not commercially available as a clinical test. Therefore, the ratios of anti-GD2 antibody to circulating GD2 and to tumor-bound GD2 have not been determined for use in our system. In ongoing clinical trials like ANBL2131, circulating GD2 levels and peak dinutuximab levels are being prospectively collected from participants throughout their treatment and may provide additional insight through correlation with clinical outcomes.

Additionally, this study was completed with a single neuroblastoma cell line and with a single anti-GD2 clone; variations are likely to arise *in vivo*, and the profundity of MFI changes may vary among cell lines. To ameliorate this weakness, we performed multiple biological replicates for each condition, separated by both space and time and normalized according to unstained controls to improve these results' generalizability. Furthermore, this *in vitro* model created a free-flowing system, in which circulating GD2 and cell-bound GD2 had equal access to the monoclonal antibodies. Using circulating GD2 and dinutuximab concentrations in patients and the GD2 binding constant of dinutuximab, our group had previously estimated that 200 nM circulating GD2 could occupy up to 95% of antibody binding sites (7). Although we observed significant decreases in antibody binding to IMR5 cells exposed to circulating GD2-LDL at higher concentrations, 5 µM GD2-LDL was required to reduce anti-GD2 antibody binding to IMR5 cells *in vitro.* Our original estimates of GD2 binding to dinutuximab in the circulation did not account for competition with antibody binding to cell surface GD2 on neuroblastoma cells. Another limitation of this study was the variability that existed among biological replicates and the use of Welch's one-way ANOVA. Although this statistical method prevented us from incurring Type 1 errors and finding false positive results, it may also have underemphasized the statistical significance of clinically important findings.

Therapeutic anti-GD2 antibodies have revolutionized the treatment of children with high-risk neuroblastoma, and medications like dinutuximab and naxitamab will continue to play critical roles in future treatment regimens. Our *in vitro* assay demonstrated that LDL-bound GD2 can interact with anti-GD2 antibodies and potentially interfere with the efficacious binding of these drugs to tumor antigens. Ongoing clinical studies should elucidate the role of circulating GD2 as a predictive biomarker of response to and efficacy of dinutuximab administered during the induction phase and could help determine the optimal timing of anti-GD2 antibody administration to ensure that children receive maximum benefit with the least amount of potentially unnecessary toxicity.

Acknowledgments

a) CST and FB would like to acknowledge with deep gratitude Alex's Lemonade Stand Foundation's Young Investigator Award and Centers of Excellence in Childhood Cancer Drug Development and Clinical Pharmacology. CST was also supported by the National Center for Advancing Translational Sciences at the University of Pennsylvania on training grant NIH NCATS TL1TR001880. d) This manuscript was originally published as a preprint: Christina S. Turn, Christine M. Busch, Cara Toland, et al. Circulating Free and Low-Density Lipoprotein-Bound GD2 Can Compete with Neuroblastoma Cells for Binding Therapeutic Anti-GD2 Antibodies. *Authorea.* April 22, 2025. CrossRef

Disclosures

Conflict of interest: Dr. Bassiri currently works at Johnson & Johnson Innovative Medicine as the an Associate Medical Director in GI Immunology but remains an adjunct faculty at the Children's Hospital of Philadelphia. The authors have no other conflicts of interest.

Financial support: This study was funded by Alex's Lemonade Stand Foundation through their Young Investigator Award program and their Centers of Excellence in Childhood Cancer Drug Development and Clinical Pharmacology. This work was also supported by NIH NCATS award TL1TR001880.

Data Availability Statement: All data from this study are available by request upon contacting the corresponding author.

Author Contributor Roles: CST: Conceptualization, investigation, funding acquisition, methodology, formal analysis, validation, visualization, writing - original draft/review & editing. CMB: Investigation, resources. CT: Investigation, resources. HB: Methodology, supervision, resources. MDH: Conceptualization, resources, supervision, writing – review & editing. FMB: Conceptualization, supervision, funding acquisition, resources, writing – review & editing

References

1. Wu ZL, Schwartz E, Seeger R, Ladisch S. Expression of GD2 ganglioside by untreated primary human neuroblastomas. Cancer Res. 1986;46(1):440-443. PubMed
2. Mohd AB, Mohd OB, Alabdallat YJ, et al. Safety and efficacy of dinutuximab in the treatment of neuroblastoma: a review. J Res Med Sci. 2023;28(1):71. CrossRef PubMed
3. Yu AL, Gilman AL, Ozkaynak MF, et al.; Children's Oncology Group. Anti-GD2 antibody with GM-CSF, interleukin-2, and isotretinoin for neuroblastoma. N Engl J Med. 2010;363(14): 1324-1334. CrossRef PubMed
4. Mody R, Naranjo A, Van Ryn C, et al. Irinotecan-temozolomide with temsirolimus or dinutuximab in children with refractory or relapsed neuroblastoma (COG ANBL1221): an open-label, randomised, phase 2 trial. Lancet Oncol. 2017;18(7):946-957. CrossRef PubMed
5. Kushner BH, Cheung IY, Modak S, et al. Humanized 3F8 anti-GD2 monoclonal antibody dosing with granulocyte-macrophage colony-stimulating factor in patients with resistant neuroblastoma: a phase 1 clinical trial. JAMA Oncol. 2018;4(12):1729-1735. CrossRef PubMed
6. Ladisch S, Wu ZL, Feig S, et al. Shedding of GD2 ganglioside by human neuroblastoma. Int J Cancer. 1987;39(1):73-76. CrossRef PubMed
7. Balis FM, Busch CM, Desai AV, et al. The ganglioside G_{D2} as a circulating tumor biomarker for neuroblastoma. Pediatr Blood Cancer. 2020;67(1):e28031. CrossRef PubMed
8. Busch CM, Balis FM. Age-dependent reference intervals in children for the disialoganglioside, G_{D2}, a circulating tumor biomarker for the childhood cancer, neuroblastoma. Clin Biochem. 2022;101:1-4. CrossRef PubMed
9. Balis FM, McCully CL, Busch CM, et al. Pharmacokinetics of the disialoganglioside, G_{D2}, a circulating tumor biomarker for neuroblastoma, in nonhuman primates. J Circ Biomark. 2021;10:26-29. CrossRef PubMed
10. Valentino LA, Ladisch S. Localization of shed human tumor gangliosides: association with serum lipoproteins. Cancer Res. 1992;52(4):810-814. PubMed
11. McNerney KO, Karageorgos S, Ferry GM, et al. TH-MYCN tumors, but not tumor-derived cell lines, are adrenergic lineage, GD2+, and responsive to anti-GD2 antibody therapy. OncoImmunology. 2022;11(1):2075204. CrossRef PubMed
12. Morini M, Barco S, Ardito M, et al. Detection of plasma circulating GD2 ganglioside in patients with neuroblastoma and age-matched healthy children. Diagnostic and prognostic evaluation. Oncologist. 2025;30(2):oyaf008. CrossRef PubMed
13. Troschke-Meurer S, Zumpe M, Ahrenberg PM, et al. Affinity affects the functional potency of anti-GD2 antibodies by target-mediated drug disposition. Cancers (Basel). 2025;17(15):2510. CrossRef PubMed
14. Kabat EA. The upper limit for the size of the human antidextran combining site. J Immunol. 1960;84(1):82-85. CrossRef PubMed
15. Desai AV, Fox E, Smith LM, et al. Pharmacokinetics of the chimeric anti-GD2 antibody, ch14.18, in children with high-risk neuroblastoma. Cancer Chemother Pharmacol. 2014;74(5): 1047-1055. CrossRef PubMed
16. Federico SM, McCarville MB, Shulkin BL, et al. A pilot trial of humanized anti-GD2 monoclonal antibody (hu14.18K322A) with chemotherapy and natural killer vells in children with recurrent/refractory neuroblastoma. Clin Cancer Res. 2017;23(21):6441-6449. CrossRef PubMed
17. Furman WL, McCarville B, Shulkin BL, et al. Improved outcome in children with newly diagnosed high-risk neuroblastoma treated with chemoimmunotherapy: updated results of a phase II study using hu14.18K322A. J Clin Oncol. 2022;40(4):335-344. CrossRef PubMed
18. Szczepanowski M, Richter J, Kehden B, et al. CD20 expression and response to rituximab treatment in B-cell precursor lymphoblastic leukemia - results of the GMALL 08/2013 Trial. Blood. 2018;132(suppl 1):1409. CrossRef
19. van Meerten T, van Rijn RS, Hol S, et al. Complement-induced cell death by rituximab depends on CD20 expression level and acts complementary to antibody-dependent cellular cytotoxicity. Clin Cancer Res. 2006;12(13):4027-4035. CrossRef PubMed
20. Reck M, Rodríguez-Abreu D, Robinson AG, et al.; KEYNOTE-024 Investigators. Pembrolizumab versus chemotherapy for PD-L1-positive non-small-cell lung cancer. N Engl J Med. 2016;375(19): 1823-1833. CrossRef PubMed
21. Herbst RS, Giaccone G, de Marinis F, et al. Atezolizumab for first-line treatment of PD-L1-selected patients with NSCLC. N Engl J Med. 2020;383(14):1328-1339. CrossRef PubMed
22. Kim SJ, Ryu KJ, Park B, et al. Exosomal and soluble programed death-ligand 1 (PD-L1) predicts responses to pembrolizumab in patients with extranodal NK/T-cell lymphoma. Cancers (Basel). 2022;14(22):5618. CrossRef PubMed
23. Sagawa R, Sakata S, Gong B, et al. Soluble PD-L1 works as a decoy in lung cancer immunotherapy via alternative polyadenylation. JCI Insight. 2022;7(1):e153323. CrossRef PubMed
24. Kurosaki T, Chamoto K, Suzuki S, et al. The combination of soluble forms of PD-1 and PD-L1 as a predictive marker of PD-1 blockade in patients with advanced cancers: a multicenter retrospective study. Front Immunol. 2023;14:1325462. CrossRef PubMed